

January 24, 2011

Measurements of Inclusive  $B \rightarrow X_u \ell \nu$  Decays

CONCEZIO BOZZI

*Istituto Nazionale di Fisica Nucleare  
Sezione di Ferrara, I-44122 Ferrara, ITALY*

*on behalf of the Babar and Belle Collaborations*

Recent results on inclusive charmless semileptonic decays of B mesons are reviewed. Emphasis is given to measurements on the recoil of fully reconstructed B mesons, which allow to exploit several regions of phase space. Preliminary averages of the CKM matrix element  $|V_{ub}|$  from the Heavy Flavour Working Group are shown, using four different theoretical calculations.

PROCEEDINGS OF CKM2010

the 6th International Workshop on the CKM Unitarity  
Triangle, University of Warwick, UK, 6-10 September 2010

# 1 Introduction

Measurements of inclusive charmless semileptonic decays of B mesons,  $B \rightarrow X_u \ell \nu$ , are directly related to the CKM matrix element  $|V_{ub}|$ . The theoretical description [1] of the hadronic current involved in these decays, relying on the Operator Product Expansion (OPE) technique, allows the determination of  $|V_{ub}|$  from the total decay rate with a small uncertainty. However, in order to suppress background from semileptonic decays with charm,  $B \rightarrow X_c \ell \nu$ , measurements of partial branching fraction are performed in restricted kinematic regions. Unfortunately, OPE breaks down in some of these regions, and the theoretical uncertainty increases significantly. Contributions due to weak annihilation also play a role in part of the kinematic regions, and need to be carefully assessed. In short, theory and background subtraction give conflicting requirements, and a trade-off must be found. Due to the improved knowledge of  $B \rightarrow X_c \ell \nu$  transitions and to the abundant data samples collected at the B factories, recent results based on phase space regions which are increasingly larger allow for an improved precision in the  $|V_{ub}|$  determinations.

Experimental measurements of charmless semileptonic decays are reviewed in Section 2, with emphasis on new preliminary results from Babar. Preliminary  $|V_{ub}|$  averages from the Heavy Flavour Averaging Group by using the available theory calculations are presented in Section 3. Conclusions are given in Section 4.

## 2 Measurements of Partial Branching Fractions

Measurements in the endpoint region of the lepton momentum spectrum are conceptually simple, being based on the identification of an high momentum lepton only. However, the kinematic region selected by the high lepton momentum requirement to suppress charmed background suffers from sizeable theoretical uncertainties. All experimental efforts [2] have been devoted to reducing the lepton momentum cut as low as allowed by background knowledge. Signal-to-background ratios (S/B) of the order of 1/10 have been achieved, with signal efficiencies at the 30% level or less. An improved analysis [3], based on the measurement of missing energy to estimate the maximum kinematically allowed hadronic mass squared,  $s_h^{max}$ , resulted in S/B of about 1/2. A summary of the available endpoint measurements is given in Table 1.

The *recoil technique* aims at fully reconstructing one of the two B mesons ( $B_{reco}$ ) from the  $\Upsilon(4S)$  decay in a fully hadronic decay, which allows to determine completely the decay kinematics of the other B ( $B_{recoil}$ ). It is therefore possible to access relevant kinematic variables, such as the invariant mass of the hadronic system,  $m_X$ , the light-cone momentum component  $P_+ = E_X - |\vec{p}_X|$ , and the squared invariant mass of the lepton pair,  $q^2$ . Semileptonic events are identified by an high-momentum lepton ( $p_\ell^* > 1$  GeV) and a missing mass consistent with zero. Non semileptonic backgrounds

| Experiment |   | $\mathcal{L}(fb^{-1})$ | $E_\ell$ (GeV) | $\Delta\mathcal{B}(10^{-4})$ |
|------------|---|------------------------|----------------|------------------------------|
| E1         | Babar                                     | 81.4                   | 2.0–2.6        | $5.72 \pm 0.41 \pm 0.65$     |
| E2         | Belle                                     | 27.0                   | 1.9–2.6        | $8.5 \pm 0.4 \pm 1.5$        |
| E3         | CLEO                                      | 9.13                   | 2.2–2.6        | $2.30 \pm 0.15 \pm 0.35$     |
| E4         | Babar ( $s_h^{max} < 3.5 \text{ GeV}^2$ ) | 81.4                   | 2.0–2.6        | $4.41 \pm 0.42 \pm 0.42$     |

Table 1: Summary of endpoint analyses, labeled E1–E4 in the following.

| Kinematic Region |    |  | Signal Yield   | $\Delta\mathcal{B}(B \rightarrow X_u \ell \nu) (10^{-3})$ |
|------------------|----|--|----------------|---|
| Babar            | R1 | $M_X < 1.55 \text{ GeV}/c$                           | $1033 \pm 73$  | $1.08 \pm 0.08 \pm 0.06$                                  |
|                  | R2 | $M_X < 1.70 \text{ GeV}/c$                           | $1089 \pm 82$  | $1.15 \pm 0.10 \pm 0.08$                                  |
|                  | R3 | $P_+ < 0.66 \text{ GeV}$                             | $902 \pm 80$   | $0.98 \pm 0.09 \pm 0.08$                                  |
|                  | R4 | R2 and $q^2 > 8 \text{ GeV}/c^2$                     | $665 \pm 53$   | $0.68 \pm 0.06 \pm 0.04$                                  |
|                  | R5 | $p_\ell^* > 1 \text{ GeV}/c, (M_X, q^2) \text{ fit}$ | $1441 \pm 102$ | $1.80 \pm 0.13 \pm 0.15$                                  |
|                  | R6 | $p_\ell^* > 1.3 \text{ GeV}/c$                       | $562 \pm 55$   | $0.76 \pm 0.08 \pm 0.07$                                  |
| Belle            | R5 | $p_\ell^* > 1 \text{ GeV}/c, (M_X, q^2) \text{ fit}$ | $1032 \pm 91$  | $1.96 \pm 0.17 \pm 0.16$                                  |

Table 2: Summary of signal yields and partial branching fractions in six kinematic regions (labeled R1–R6 in the following). Unless otherwise noted, the lepton momentum in the center-of-mass frame is required to be  $p_\ell^* > 1 \text{ GeV}/c$ . The uncertainty on the yields is statistical only.

are subtracted by studying the distribution of the beam-energy substituted mass  $m_{ES}$  for the  $B_{reco}$  candidates. About 1000 hadronic modes are reconstructed, with efficiencies at the 0.3% (0.5%) level for neutral (charged) B decays.

Background from  $B \rightarrow X_c \ell \nu$  is reduced mainly by vetoing charged kaons and  $K_S$ , whose production is highly suppressed in signal, and charged and neutral soft pions kinematically compatible with  $B \rightarrow D^* \ell \nu$  decays.

Both B Factory experiments published results using the recoil technique [4]. Babar recently released [5] a preliminary update based on the full dataset ( $426 \text{ fb}^{-1}$ ), which is detailed in the following. The integrated luminosity analysed by Belle is  $626 \text{ fb}^{-1}$ .

Partial rates for charmless semileptonic decays have been measured in several phase space regions, defined in Table 2, as well as for charged and neutral  $B$  decays separately. The latter is achieved by explicitly requiring the (absolute)  $B_{reco}$  charge to be one or zero, respectively, after subtracting with Monte Carlo a small fraction of events where the  $B_{reco}$  charge was not correctly reconstructed. In addition to the  $m_X$ ,  $P_+$  and  $(m_X, q^2)$  distributions, the lepton momentum  $p_\ell^*$  was also studied. A background-enriched control sample, obtained by reversing the vetoes on kaons and soft pions mentioned above, was used to determine the relative contribution due to semileptonic decays into P-wave D mesons directly on data; Monte-Carlo simulation

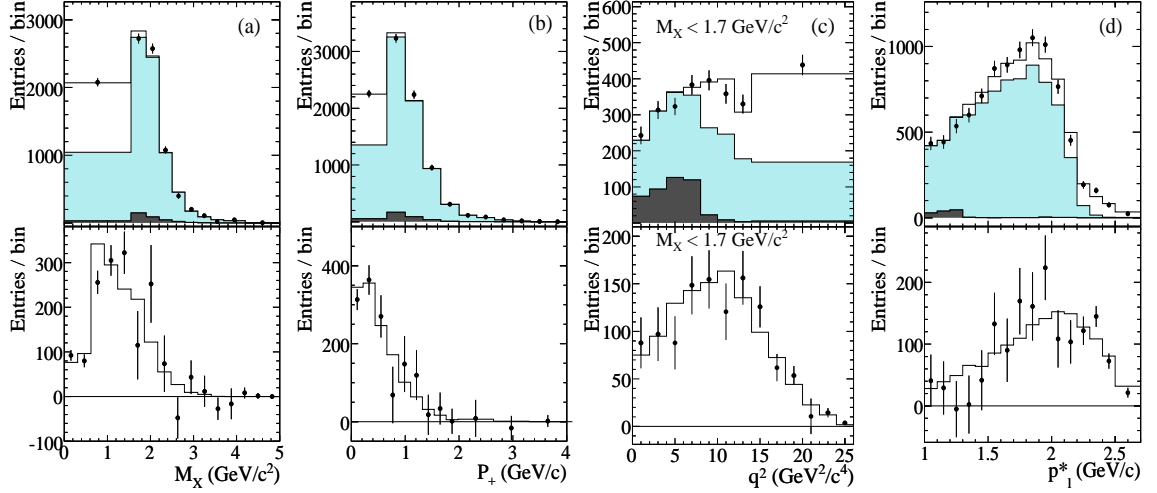


Figure 1: Upper row:  $M_X$  (a),  $P_+$  (b),  $q^2$  with  $M_X < 1.7 \text{ GeV}/c^2$  (c) and  $p_\ell^*$  (d) spectra (data points), measured in Babar data. The result of the fit to the sum of three MC contributions is shown in the histograms:  $B \rightarrow X_u \ell \nu$  decays generated inside (no shading) and outside (dark shading) the selected kinematic region, and  $B \rightarrow X_c \ell \nu$  and other background (light shading). Lower row: corresponding spectra for  $B \rightarrow X_u \ell \nu$  (not corrected for efficiency) after background subtraction.

was then reweighted accordingly. Although the impact on signal yields was almost negligible, the fit chisquares improved significantly.

The event yields and partial branching fractions are given in Table 2. The distributions of the kinematic variables under study, before and after background subtraction, are shown in Figure 1. Statistical uncertainties range from 7% to 9%.

A summary of the systematic uncertainties is given in Table 3, which also shows the corresponding uncertainties from the Belle recoil analysis. The statistical and experimental systematic uncertainties are of the same order. Detector-related uncertainties are dominated by undetected or mismeasured particles (*e.g.*  $K_L$  and additional neutrinos) from background. Progress on the knowledge of exclusive  $B \rightarrow X_c \ell \nu$  decays reflects in a relatively small uncertainty due to background composition. In the most inclusive phase space region (R5), the dominant uncertainty is due to the signal model, in particular to the knowledge of heavy quark parameters and the branching fraction of exclusive  $B \rightarrow X_u \ell \nu$  decays, which are used in the simulation to determine signal efficiency. Total uncertainties range between 9% and 13%.

Measurements of partial rates for charged and neutral  $B$  mesons allow to determine the relative contribution of weak annihilation to the total rate,  $\gamma_{WA}/\Gamma$ . The resulting 90% confidence level regions are reported in Table 4; they are in agreement with previous determinations [6].

| Source             | Babar       |               |               |               |               |               | Belle      |
|--------------------|-------------|---------------|---------------|---------------|---------------|---------------|------------|
|                    | R1          | R2            | R3            | R4            | R5            | R6            | R5         |
| Statistical error  | 7.1         | 8.9           | 8.9           | 8.0           | 7.1           | 8.9           | 8.8        |
| MC statistics      | 1.3         | 1.3           | 1.3           | 1.6           | 1.1           | 1.2           |            |
| Detector-related:  | 2.8         | 3.7           | 5.5           | 4.1           | 3.2           | 2.7           | 3.3        |
| Fit-related:       | 2.7         | 4.9           | 3.2           | 3.2           | 2.1           | 2.5           | 3.6        |
| Signal model:      | 2.7         | 3.0           | 3.5           | 1.9           | 6.6           | 7.9           | 6.3        |
| Background model:  | 2.0         | 2.6           | 3.4           | 2.8           | 2.8           | 2.2           | 1.7        |
| Total systematics: | 5.3<br>-5.0 | 6.4<br>-6.2   | 8.0<br>-8.1   | 6.2<br>-6.2   | 8.5<br>-7.7   | 9.4<br>-8.7   | $\pm 8.1$  |
| Total error:       | 9.0<br>-8.8 | 11.0<br>-10.9 | 12.0<br>-12.1 | 10.2<br>-10.3 | 11.1<br>-10.5 | 12.9<br>-12.4 | $\pm 12.0$ |

Table 3: Systematic uncertainties (in percent) on the partial branching fractions for the various phase space regions, for the Babar and Belle recoil analyses.

### 3 $|V_{ub}|$ determinations

The value of  $|V_{ub}|$  is related to the measured partial branching fractions by

$$|V_{ub}| = \sqrt{\frac{\Delta\mathcal{B}(B \rightarrow X_u \ell \nu)}{\tau_B \cdot \Delta\Gamma_{theory}}}, \quad (1)$$

where the  $B \rightarrow X_u \ell \nu$  width according to the applied cuts,  $\Delta\Gamma_{theory}$ , and its uncertainty are determined by four theoretical calculations [8, 9, 10, 11]. Theoretical uncertainties can be divided in parametric terms, due to uncertainties on heavy quark parameters and  $\alpha_s$ , and non-parametric contributions due, for instance, to higher order terms in the heavy quark expansion, weak annihilation, leading and subleading shape functions, renormalization scale.

The procedure for performing the averages is documented in [7]. The average B lifetime used is 1.578 ps. The input values for the heavy quark parameters have been determined by a global fit in the kinetic scheme, translated to the scheme needed by

| Phase Space Region | $(R^{+/0} - 1)$              | 90% C.L. on $\gamma_{WA}/\Gamma$ |
|--------------------|------------------------------|----------------------------------|
| R1                 | $-0.020 \pm 0.066 \pm 0.003$ | $[-0.13, 0.09]$                  |
| R2                 | $0.071 \pm 0.117 \pm 0.011$  | $[-0.12, 0.26]$                  |
| R4                 | $0.042 \pm 0.066 \pm 0.009$  | $[-0.07, 0.15]$                  |
| R5                 | $0.109 \pm 0.157 \pm 0.019$  | $[-0.15, 0.37]$                  |

Table 4: Results for  $(R^{+/0} - 1)$  and limits on  $\gamma_{WA}/\Gamma$  for the various kinematic regions under study by Babar.

| Kin.<br>region       | Expt. | BLNP<br>[8]                     | DGE<br>[9]                      | GGOU<br>[10]                    | ADFR<br>[11]                    |
|----------------------|-------|---------------------------------|---------------------------------|---------------------------------|---------------------------------|
| Endpoint analyses    |       |                                 |                                 |                                 |                                 |
| E1                   | Babar | $4.35 \pm 0.25^{+0.31}_{-0.30}$ | $4.15 \pm 0.28^{+0.28}_{-0.25}$ | $4.17 \pm 0.24^{+0.20}_{-0.33}$ | $3.98 \pm 0.27^{+0.24}_{-0.25}$ |
| E2                   | Belle | $4.81 \pm 0.45^{+0.32}_{-0.29}$ | $4.66 \pm 0.43^{+0.26}_{-0.25}$ | $4.65 \pm 0.43^{+0.19}_{-0.30}$ | $4.53 \pm 0.42^{+0.27}_{-0.27}$ |
| E3                   | CLEO  | $4.00 \pm 0.47^{+0.34}_{-0.34}$ | $3.70 \pm 0.43^{+0.30}_{-0.26}$ | $3.81 \pm 0.44^{+0.22}_{-0.39}$ | $3.47 \pm 0.41^{+0.21}_{-0.22}$ |
| E4                   | Babar | $4.48 \pm 0.30^{+0.39}_{-0.37}$ | $4.15 \pm 0.28^{+0.30}_{-0.30}$ | n.a.                            | $3.87 \pm 0.26^{+0.24}_{-0.24}$ |
| Sim.ann.             | Belle | $4.39 \pm 0.46^{+0.31}_{-0.29}$ | $4.30 \pm 0.45^{+0.24}_{-0.23}$ | $4.24 \pm 0.45^{+0.25}_{-0.33}$ | $3.94 \pm 0.41^{+0.23}_{-0.24}$ |
| Recoil Analyses      |       |                                 |                                 |                                 |                                 |
| R1                   | Babar | $4.03 \pm 0.19^{+0.28}_{-0.26}$ | $4.23 \pm 0.20^{+0.22}_{-0.19}$ | $3.96 \pm 0.18^{+0.24}_{-0.27}$ | $3.86 \pm 0.18^{+0.24}_{-0.25}$ |
| R2                   | Babar | $3.92 \pm 0.22^{+0.25}_{-0.23}$ | $4.04 \pm 0.22^{+0.26}_{-0.23}$ | $3.84 \pm 0.21^{+0.17}_{-0.20}$ | $3.78 \pm 0.21^{+0.23}_{-0.24}$ |
| R3                   | Babar | $3.90 \pm 0.24^{+0.28}_{-0.26}$ | $3.93 \pm 0.24^{+0.36}_{-0.29}$ | $3.64 \pm 0.22^{+0.30}_{-0.30}$ | $3.60 \pm 0.22^{+0.23}_{-0.24}$ |
| R4                   | Babar | $4.22 \pm 0.22^{+0.30}_{-0.28}$ | $4.10 \pm 0.22^{+0.23}_{-0.22}$ | $4.07 \pm 0.22^{+0.24}_{-0.32}$ | $3.78 \pm 0.20^{+0.23}_{-0.23}$ |
| R5                   | Babar | $4.27 \pm 0.24^{+0.23}_{-0.20}$ | $4.34 \pm 0.24^{+0.15}_{-0.15}$ | $4.29 \pm 0.24^{+0.11}_{-0.14}$ | $4.34 \pm 0.24^{+0.15}_{-0.15}$ |
| R6                   | Babar | $4.22 \pm 0.27^{+0.23}_{-0.21}$ | $4.27 \pm 0.27^{+0.16}_{-0.16}$ | $4.21 \pm 0.27^{+0.12}_{-0.16}$ | $4.28 \pm 0.27^{+0.26}_{-0.25}$ |
| R5                   | Belle | $4.45 \pm 0.27^{+0.24}_{-0.21}$ | $4.53 \pm 0.27^{+0.15}_{-0.15}$ | $4.47 \pm 0.27^{+0.11}_{-0.15}$ | $4.55 \pm 0.30^{+0.27}_{-0.27}$ |
| Average              |       | $4.30 \pm 0.16^{+0.21}_{-0.23}$ | $4.37 \pm 0.15^{+0.17}_{-0.16}$ | $4.30 \pm 0.16^{+0.13}_{-0.20}$ | $4.05 \pm 0.13^{+0.24}_{-0.21}$ |
| $\chi^2/d.o.f.$ (CL) |       | 12.2/11 (0.36)                  | 7.52/11 (0.76)                  | 12.2/10 (0.27)                  | 28.2/11 (0.003)                 |

Table 5: Results for  $|V_{ub}|$  obtained with four theoretical calculations. The uncertainties are experimental (*i.e.* sum of statistical and experimental systematical) and theoretical, respectively. The phase space regions are defined in Tables 1 and 2.

each model, where both  $b \rightarrow c\ell\nu$  and  $b \rightarrow s\gamma$  moments are used, giving  $m_b(kin) = 4.591 \pm 0.031$  GeV,  $\mu_\pi^2(kin) = 0.454 \pm 0.038$  GeV<sup>2</sup>, and a correlation of -40.5%.

Preliminary averages from the Heavy Flavour Working Group are shown in Table 5, for the four available theoretical calculations. All methods give consistent results and comparable uncertainties.

A recent NNLO calculation [12] of the leading term in the partial rates gives a surprising change with respect to the NLO calculation used in the BLNP method, therefore suggesting an underestimate of the theoretical uncertainty due to the renormalization matching scale. The corresponding change in  $|V_{ub}|$  is of the order of 8%. Similar estimates for the other methods are not available yet. This effect has not been taken into account in the current  $|V_{ub}|$  determinations.

## 4 Conclusion

Several  $|V_{ub}|$  determinations from measurements of inclusive spectra on the full data sets collected at the B Factories are now available. In the most inclusive kinematic regions, the dominant error is due to uncertainties in signal modeling, which directly propagate in the selection efficiency. This uncertainty can be reduced by applying stricter kinematic cuts, but theoretical uncertainties correspondingly increase. Back-

ground modeling dominates endpoint analyses. Statistical and systematic uncertainties on the partial rates are comparable. Contributions due to weak annihilation are now being addressed with data; however, the statistical sensitivity is still beyond theoretical expectations.

The uncertainty on inclusive  $|V_{ub}|$  determinations is at the 6% level, dominated by parametric errors (4% from a 40 MeV uncertainty on the  $b$  quark mass). Determinations by using the four available calculations are consistent between each other; all methods give comparable theory uncertainties, and the spread among calculations is comparable to theory errors. Recent results on NNLO calculations might hint to an underestimate of non-parametric theory uncertainties, which needs to be clarified.

## References

- [1] a comprehensive and critical review of the theoretical framework and calculations is given by Einan Gardi in these Proceedings.
- [2] A. Bornheim et al. (CLEO Collaboration), Phys. Rev. Lett. 88, 231803 (2002)  
B. Aubert et al. (BABAR Collaboration), Phys. Rev. D 73, 012006 (2006)  
A. Limosani et al. (Belle Collaboration), Phys. Lett. B 621, 28 (2005)
- [3] B. Aubert et al. (BABAR Collaboration), Phys. Rev. Lett. 95, 111801 (2005)
- [4] B. Aubert et al. (BABAR Collaboration), Phys. Rev. Lett. 100, 171802 (2008)  
P. Urquijo et al. (Belle Collaboration), Phys. Rev. Lett. 104, 021801 (2010)
- [5] M. Sigamani, in proceedings of the 35th International Conference on High Energy Physics, PoS(ICHEP 2010)265
- [6] J. L. Rosner et al. (CLEO Collaboration), Phys. Rev. Lett. 96, 121801 (2006)  
B. Aubert et al. (BABAR Collaboration), arXiv:0708.1753v1 [hep-ex]
- [7] D. Asner et al. (The Heavy Flavor Averaging Group), arXiv:1010.1589v1 [hep-ex]
- [8] B.O. Lange, M. Neubert and G. Paz, Phys. Rev. D72, 073006 (2005) and references therein
- [9] J.R. Andersen and E. Gardi, JHEP 0601, 097 (2006), updated in arXiv:0806.4524
- [10] P. Gambino, P. Giordano, G. Ossola, and N. Uraltsev, JHEP 0710, 058 (2007)
- [11] U. Aglietti, F. Di Lodovico, G. Ferrera, and G. Ricciardi, Eur. Phys. J. C59, 831 (2009) and references therein
- [12] C. Greub, M. Neubert, B.D. Pecjak, Eur. Phys. J. C65, 501 (2010)